

## One-way coupling enables noise-mediated spatiotemporal patterns in media of otherwise quiescent multistable elements

John F. Lindner<sup>1</sup> and Adi R. Bulsara<sup>2</sup>

<sup>1</sup>Physics Department, The College of Wooster, Wooster, Ohio 44691, USA

<sup>2</sup>Space and Naval Warfare Systems Center, Code 2373, 53560 Hull Street, San Diego, California 92152, USA

(Received 12 October 2005; revised manuscript received 20 March 2006; published 28 August 2006)

Recent work has demonstrated that *undriven* and *overdamped* bistable systems, which are normally quiescent, can oscillate if unidirectionally coupled into arrays with cyclic boundary conditions. Here, we understand such oscillations as corresponding to the propagation of solitonlike waves. Further, in large arrays, we demonstrate how noise and coupling, together, mediate the resulting complex spatiotemporal dynamics.

DOI: [10.1103/PhysRevE.74.020105](https://doi.org/10.1103/PhysRevE.74.020105)

PACS number(s): 05.40.-a, 05.45.-a, 89.75.Kd, 05.10.-a

Noise-mediated spatiotemporal phenomena are important in many fields [1]; in particular, thermal and noise-induced pattern formation has recently been studied extensively [2]. Recent work has characterized spatially and temporally disordered states in the complex Ginzburg-Landau equation, both with and without noise [3], and has explored the propagation of solitons, pulses, and excitable structures in bistable media [4].

Noise and coupling-induced oscillations in arrays of overdamped bistable elements have been studied in two related nonlinear phenomena: array-enhanced stochastic resonance [5] and array-enhanced coherence resonance [6]. In the former, noise and coupling that maximize the local response of bistable elements to external subthreshold time-periodic signals also facilitate their global spatiotemporal synchronization. In the latter, noise and coupling in excitable systems generate a quasiregular response even in the absence of an external signal. It is also well known that undriven overdamped bistable systems do not oscillate. However, recent work demonstrates that cyclic arrays (or rings) of such systems can oscillate if they are unidirectionally coupled, provided the coupling strength exceeds a critical value [7,8].

These oscillations, which correspond to the individual dynamic elements hopping between two or more stable states, can be understood as resulting from coupling-induced Hopf bifurcations, if one construes the arrays as higher-dimensional dynamical systems. Instead, in this work, we understand the oscillations as resulting from a “frustrated” equilibrium, where solitonlike waves of dislocations (shifts, defects) in equilibria propagate endlessly around rings of unidirectionally coupled bistable elements. We then study the effects of noise on the propagation of these solitons [9] and on the complex spatiotemporal dynamics that emerges from the consequent interplay among noise, coupling, and nonlinear dynamics.

Our results apply to any nonlinear overdamped elemental dynamics  $dx/dt = -\nabla_x U$  with a multistable potential energy function  $U[x]$ . For concreteness, we focus on a specific device, the fluxgate magnetometer, which was the subject of our earlier work [8], and whose core dynamics can be characterized by the potential [10]

$$U[x] = \frac{1}{2}x^2 - \frac{1}{c} \ln[\cosh[cx]], \quad (1)$$

where  $x[t]$  denotes the (suitably normalized) core magnetization. The system bistability, evident from a small  $x$  expansion of (1), is controlled by the (temperature-dependent) parameter  $c$ . At temperatures above the Curie point,  $c < 1$  corresponding to monostability and a paramagnetic core, whereas for  $c > 1$ , the potential is bistable corresponding to a ferromagnetic core.

Rings of a small (and odd) number of such ferromagnetic cores are now being incorporated into coupled-core fluxgate magnetometers for sensitive magnetic field measurements [11]. The coupled-core dynamics [8] follows from the potential (1), and obeys

$$\tau_F \frac{dx_n}{dt} = -x_n + \tanh[c(x_n + \lambda x_{n+1} + \epsilon)] + \xi_n, \quad (2)$$

where  $x_n[t]$  denotes the magnetization of the  $n$ th core,  $\epsilon[t]$  is a (typically very weak) target signal,  $\tau_F$  is the (typically small) device time constant, and  $\lambda$  is the coupling strength. Note that the coupling is one way: element  $n$  is coupled to element  $n+1$ , but not to element  $n-1$ . The Gaussian noise  $\xi_n[t]$  has zero mean and exponential correlation  $\langle \xi_n[t_1] \xi_m[t_2] \rangle = \delta_{nm} \sigma^2 \exp[-|t_1 - t_2|/\tau]$ , with variance  $\sigma^2$ , correlation time  $\tau$ , and noise intensity  $D = \sigma^2 \tau$ . While the noise is correlated in time (or “colored”) at each site, it is independent from site to site. We realize the ring topology by identifying the elements  $n=1$  and  $n=N+1$ .

For simplicity, we measure time in units of the device time constant, taking  $\tau_F = 1$  in Eq. (2). We assume a vanishing signal  $\epsilon=0$  so that all the single-core potentials are *a priori* symmetric, choose the nonlinearity  $c=3$  to ensure the bistability of each element in the absence of coupling, and fix the noise correlation time at  $\tau=1$  (unless otherwise stated), while varying the noise intensity  $D$  and the coupling strength  $\lambda$ .

The noise intensity  $D$  is best expressed in units of the single-element energy barrier height  $\Delta V$ , while  $\lambda$  is best expressed in units of the critical coupling  $\lambda_c$ , below which the noiseless ring oscillates. A straightforward calculation yields [10]  $\Delta V = 0.2698$ , while the critical coupling is readily calcu-

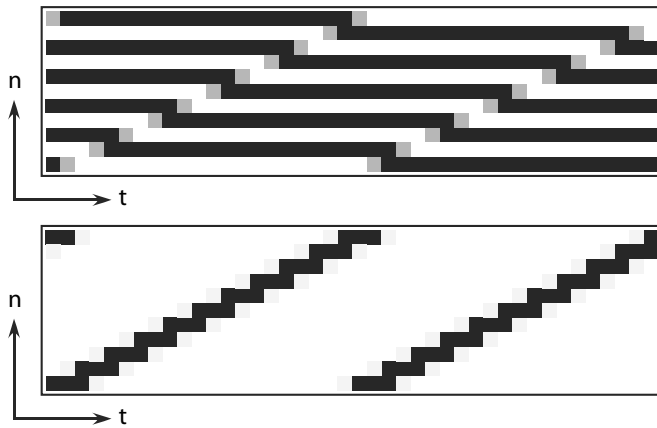


FIG. 1. Generic spatiotemporal evolution of a noiseless ring of  $N=11$  unidirectionally coupled bistable elements. After a short transient from random initial conditions, neighboring elements equilibrate by alternately pushing and pulling each other into opposite potential wells—except for one leftover coupling, which propagates endlessly as an alternating push and pull. In the top plot of states  $x_n[t]$ , white represents one well and black the other, with grays in between. In the bottom plot of filtered states  $\Delta x_n[t]$ , dark grays emphasize departures from spatial alternation and temporal stationarity.

lated [8] via the prescription  $\lambda_c = -x_i + c^{-1} \tanh^{-1} x_i$  with  $x_i = \sqrt{(c-1)/c}$ . We concentrate, initially, on the regime  $\lambda/\lambda_c > 0$ , for which the ring tends toward an “antiferromagnetic” equilibrium [12], wherein adjacent elements are in opposite states; the  $\lambda/\lambda_c < 0$  case, for which the ring tends toward a “ferromagnetic” equilibrium, wherein adjacent elements are in similar states, is discussed later. Finally, we numerically integrate the system of Eq. (2) using the Euler-Maruyama algorithm [13] with a typical integration time step of  $dt=0.004$ .

Our space-time plots of the evolution of the arrays represent the positions of each of the elements with a shade of gray, where black represents one potential well and white the other and intermediate grays interpolate between. The arrays tend toward an equilibrium in which neighboring elements are alternately in opposite wells, and this produces horizontal striped patterns that are distracting to the eye. Hence, most of our figures are graphically filtered to emphasize departures from spatial (vertical) alternation and temporal (horizontal) stationarity. We introduce the filtered dynamics

$$\Delta x_n[t] = \alpha(x_{n+1}[t] - x_{n-1}[t])^\gamma + \beta(x_n[t+dt] - x_n[t])^\gamma, \quad (3)$$

where the parameters  $\alpha$ ,  $\beta$ , and  $\gamma$  are chosen to produce clear images of the moving dislocations, as demonstrated in Fig. 1 with  $\alpha=0.1$ ,  $\beta=0.1$ , and  $\gamma=4$ . Furthermore, as each soliton divides the array into two quiescent, equilibrated domains, we color the domains alternately red and cyan for clarity, as in Fig. 2. The space-time plots in all our figures present the time increasing toward the right and the element number increasing toward the top. Since element  $N$  is coupled to element 1, the plots embody the vertical periodic boundary condition, and consequently, can be wrapped into horizontal cylinders or tiled vertically.

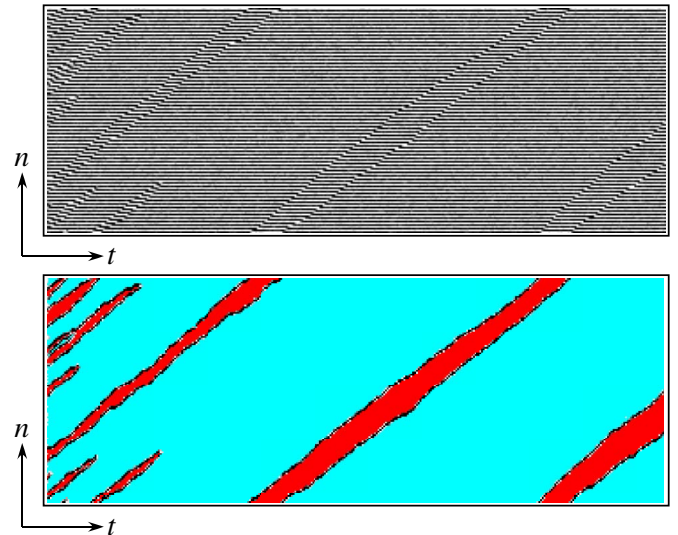


FIG. 2. (Color online) Spatiotemporal evolution of a moderately noisy ring of  $N=128$  unidirectionally coupled bistable elements, after a short transient from random initial conditions. Top plot represents the unfiltered positions of the elements, bottom plot is filtered, as in Fig. 1, to emphasize the dislocations, and colored to readily distinguish the domains bounded by the dislocations. Noise intensity is  $D=0.185\Delta V$  and coupling is  $\lambda=2\lambda_c$ .

With no noise and random initial conditions, the arrays rapidly evolve toward a global equilibrium in which neighboring bistable elements are alternately forced into opposite stable potential wells, as they alternately push and pull each other. For rings with an odd number of elements, the approach to global equilibrium is frustrated, since there is always at least one unpaired coupling that propagates around and around the ring as an alternating push and pull in coupling and a shift or dislocation in equilibrium, like the soliton of Fig. 1. Each element periodically shifts as the soliton passes through it, with a frequency equal to the ratio of the ring circumference to the soliton speed (which increases with coupling strength). For rings with an even number of elements, there is no unpaired coupling, and the entire ring equilibrates to quiescence—given sufficient time. However, if the ring is large, distant and essentially independent solitons can arise from random initial conditions and propagate at virtually the same speed—forming parallel worldlines in the space-time plots—leading to *extremely* long transients, where elements continue to periodically shift wells for very long times when the dislocations pass through them. The latter behavior is realized only in large ( $N \gtrsim 100$ ) arrays.

Figure 3 illustrates the filtered spatiotemporal evolution from random initial conditions of a ring of  $N=127$  overdamped bistable elements, as a function of coupling and noise, after a transient evolution of duration  $t \sim 10^4 \tau_F$ . The first (bottom) row illustrates the evolution of noiseless rings for four different coupling strengths. Strong antiferromagnetic coupling  $\lambda/\lambda_c > 1$  forces adjacent elements into opposite states (rendered as white in the filtered plots) except at dislocations that chase each other around the ring at a constant speed. Weak antiferromagnetic coupling  $0 < \lambda/\lambda_c < 1$  is unable to move the elements from their random initial states.

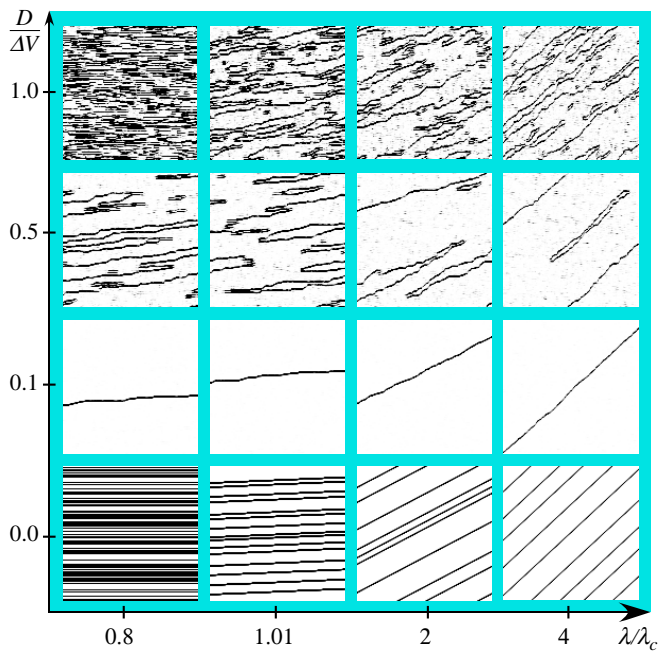


FIG. 3. (Color online) The filtered spatiotemporal evolution of a ring of  $N=127$  unidirectionally coupled bistable elements during a time  $\Delta T \sim 10^2 \tau_F$ , as a function of coupling  $\lambda$  (horizontal) and noise intensity  $D$  (vertical). In all cases, a long transient of duration  $t \sim 10^4 \tau_F$  has been omitted. Within each panel, the time  $t$  increases rightward and the element number  $n$  increases upward. The slopes of the soliton worldlines increase rightward, as the soliton speeds increase with coupling.

Large coupling increases the speed of hopping from one well to the next and thereby increases the mean speed of the solitons. Similar behavior is obtained for a noiseless ring with an even number of elements.

Adding even a small amount of noise, as in the second row of Fig. 3, dramatically changes the dynamics by perturbing the worldlines of the dislocations and causing them to wander, collide, and annihilate each other. For a ring with an odd number of elements, this leaves a single, solitary dislocation moving around the ring, causing every element to shift from one of its stable states to the other once each circumnavigation, keeping the ring quiet except at the moving dislocation. For a ring with an even number of elements, all the dislocations eventually collide and annihilate each other in pairs, leaving the ring quiet, except for the small noise. The distinction between sub- and supercritical dynamics is blurred, as the behavior for  $\lambda$  just below the critical coupling  $\lambda_c$  is similar to the behavior just above.

For moderate noise, as in the third row of Fig. 3, a new capability emerges, as noise not only annihilates pairs of dislocations, but it also creates them, forming closed loops in the space-time diagrams. The elements of the ring are oscillating but no longer at the same frequency. Finally, for any given coupling, sufficient noise can overwhelm the domains of order segregated by the dislocation waves, as in the left panel of the fourth row of Fig. 3.

The spatiotemporal evolution (not shown) of an  $N=128$  ring of overdamped bistable elements is very similar to that of the  $N=127$  ring summarized in Fig. 3, except that the

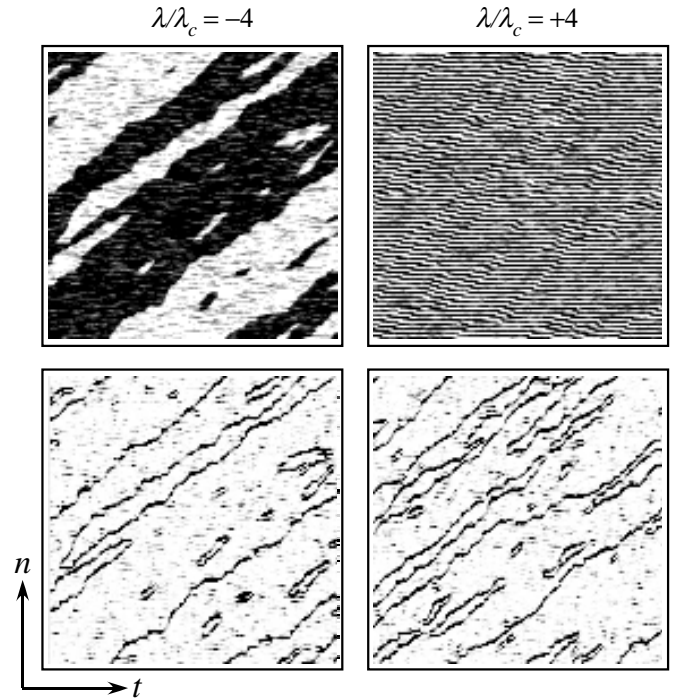


FIG. 4. Spatiotemporal evolution of a ring of  $N=127$  elements for positive and negative coupling at large noise intensity  $D=\Delta V$ . Top row is unfiltered; bottom row is filtered. The domain structures are qualitatively similar.

second row is blank, corresponding to the complete annihilation (in pairs) of all the solitons.

Interestingly, although the spatiotemporal dynamics of antiferromagnetic coupling  $\lambda/\lambda_c > 0$  is superficially very different from that of ferromagnetic coupling  $\lambda/\lambda_c < 0$ , as demonstrated in the unfiltered images of the top row of Fig. 4, the emergent domain structures are similar, as revealed in the filtered images of the bottom row.

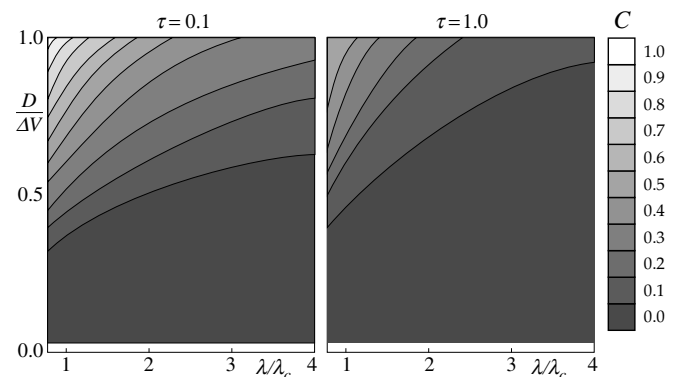


FIG. 5. Contour plots of the complexity  $C$  of the spatiotemporal evolution of a ring of  $N=127$  elements during a time  $\Delta T=65\tau_F$ , as a function of coupling  $\lambda$  (horizontal) and noise intensity  $D$  (vertical), for two values of noise correlation time  $\tau$ . In all cases, a long transient of  $t=4000\tau_F$  has been omitted. Small coupling, large noise intensity, and small noise correlation time increase the complexity. (For simplicity, and unlike Fig. 3, the exceptional noiseless  $D=0$  cases are omitted here.)

As a first attempt to quantify the complexity of the spatiotemporal patterns, we introduce

$$C = \langle \Delta x_n[t] \rangle, \quad (4)$$

the space-time average of the filtered dynamics  $\Delta x_n[t]$ , which we plot in Fig. 5 as a function of coupling and noise intensity, for two different noise correlation times. The metric  $C$  faithfully reflects the complexity of the spatiotemporal patterns of Fig. 3. Increasing the coupling at constant noise intensity tends to reduce complexity by homogenizing the array. Increasing the noise correlation time tends to reduce the complexity by resisting rapid changes.

In conclusion, we have elucidated the mechanism of emergent oscillations in rings of unidirectionally coupled bistable elements by describing them in terms of a topologically frustrated approach to equilibrium. The one-way coupling breaks the rotational symmetry of the ring by allowing information to flow in only one direction, and then noise and coupling, together, induce complex and subtle spatiotemporal dynamics, democratizing the dynamics above and below the critical coupling and between rings with even and odd numbers of elements. It is important to note that, in experi-

ments, the coupled system draws energy from the electronics used to realize the coupling circuits [11], so that no fundamental laws are violated, even in the absence of a deterministic forcing signal.

While previous work [8,11] with noiseless arrays focused on oscillations in rings with an odd number of elements, we show here that, in the presence of noise, the spatiotemporal behavior of rings with an even number of elements is comparably interesting, although quite different, particularly at low  $N$  and low noise. Indeed, if the extremely long transients in even- $N$  rings are vulnerable to weak deterministic external signals, the rate of their extinction might be the basis of new types of sensitive detectors. In this regard, we reiterate our expectation that the spatiotemporal behavior described in this work will occur in a wide class of coupled nonlinear systems, whose individual (uncoupled) elements are described by a multistable potential energy function.

J.F.L. thanks The College of Wooster for making possible his sabbatical at Georgia Tech. A.R.B. acknowledges support from the Office of Naval Research, Physics Division. We thank Visarath In and Ted Heath for helpful discussions.

- 
- [1] M. Loecher, *Noise Sustained Patterns* (World Scientific, Singapore, 2002).
- [2] M. Santagiustina, P. Colet, M. San Miguel, and D. Walgraef, *Phys. Rev. E* **58**, 3843 (1998); R. J. Deissler, *J. Stat. Phys.* **54**, 1459 (1989).
- [3] G. D. Granzow and H. Riecke, *Phys. Rev. Lett.* **87**, 174502 (2001); H. Wang, *Phys. Rev. Lett.* **93**, 154101 (2004).
- [4] R. H. Enns and D. E. Edmundson, *Phys. Rev. A* **47**, 4524 (1993); J. García-Ojalvo, F. Sagués, J. M. Sancho, and L. Schimansky-Geier, *Phys. Rev. E* **65**, 011105 (2001); J. García-Ojalvo and L. Schimansky-Geier, *J. Stat. Phys.* **101**, 473 (2000).
- [5] J. F. Lindner, B. K. Meadows, W. L. Ditto, M. E. Inchiosa, and A. R. Bulsara, *Phys. Rev. Lett.* **75**, 3 (1995); *Phys. Rev. E* **53**, 2081 (1996).
- [6] B. Hu and C. Zhou, *Phys. Rev. E* **61**, R1001 (2000); C. Zhou, J. Kurths, and B. Hu, *Phys. Rev. Lett.* **87**, 098101 (2001).
- [7] V. In, A. Kho, J. D. Neff, A. Palacios, P. Longhini, and B. K. Meadows, *Phys. Rev. Lett.* **91**, 244101 (2003).
- [8] V. In, A. R. Bulsara, A. Palacios, P. Longhini, A. Kho, and J. D. Neff, *Phys. Rev. E* **68**, 045102(R) (2003); A. R. Bulsara, V. In, A. Kho, P. Longhini, A. Palacios, W. J. Rappel, J. Acebron, S. Baglio, and B. Ando, *Phys. Rev. E* **70**, 036103 (2004); V. In, A. Palacios, A. Bulsara, P. Longhini, A. Kho, J. Neff, S. Baglio, and B. Ando, *Phys. Rev. E* **73**, 066121 (2006).
- [9] We use the term “soliton” in the general sense of a wavelike disturbance that propagates for long times while maintaining its shape.
- [10] A. R. Bulsara, C. Seberino, L. Gammaitoni, M. F. Karlsson, B. Lundqvist, and J. W. C. Robinson, *Phys. Rev. E* **67**, 016120 (2003).
- [11] V. In, V. Sacco, A. Kho, S. Baglio, B. Ando, A. Bulsara, and A. Palacios, *IEEE Sensors* (to be published).
- [12] The “ferromagnetic” equilibria are not related to the fluxgate’s ferromagnetic core and similar results obtained for any bistable potential.
- [13] P. E. Kloeden and E. Platen, *Numerical Solutions of Stochastic Differential Equations* (Springer, Berlin, 1992).